Wave Propagation in a Volume Hologram with Multiple Diffraction Gratings

Steven J. Frederick

Francis Marion University

Florence, SC

Advisor: Dr Boris Zeldovich

College of Optics and Photonics/Creol

University of Central Florida

Report Documentation Page

Form Approved
OMB No. 0704-0188

1. REPORT DATE	2. REPORT TYPE	3. DATES COVERED
10 AUG 2004	**N/A**	**-**

4. TITLE AND SUBTITLE	5a. CONTRACT NUMBER
Wave Propagation in a Volume Hologram with Multiple Diffraction Gratings	5b. GRANT NUMBER
	5c. PROGRAM ELEMENT NUMBER
6. AUTHOR(S)	5d. PROJECT NUMBER
	5e. TASK NUMBER
	5f. WORK UNIT NUMBER
7. PERFORMING ORGANIZATION NAME(S) AND ADDRESS(ES) **Francis Marion University Florence, SC;**	8. PERFORMING ORGANIZATION REPORT NUMBER
9. SPONSORING/MONITORING AGENCY NAME(S) AND ADDRESS(ES)	10. SPONSOR/MONITOR'S ACRONYM(S)
	11. SPONSOR/MONITOR'S REPORT NUMBER(S)

12. DISTRIBUTION/AVAILABILITY STATEMENT
Approved for public release, distribution unlimited

13. SUPPLEMENTARY NOTES
See also ADM001691, Phase Conjugation for High Energy Lasers., The original document contains color images.

14. ABSTRACT

15. SUBJECT TERMS

16. SECURITY CLASSIFICATION OF:			17. LIMITATION OF ABSTRACT	18. NUMBER OF PAGES	19a. NAME OF RESPONSIBLE PERSON
a. REPORT	b. ABSTRACT	c. THIS PAGE			
unclassified	**unclassified**	**unclassified**	**UU**	**23**	

Abstract

In the last 10 years, Bragg diffraction gratings have been developed at CREOL using photo-thermo-refractive (PTR) glass, which is not sensitive to radiation, temperatures to 400°C, and can withstand high intensity laser beams without damage or change in the Bragg angle. In this work, a new type of Bragg grating, not yet fabricated, is being studied to predict its properties. It is composed of two gratings in the same material, at 90 degrees to each other and 45 degrees to the incident wave. By solving equations that relate to wave propagation through this grating, it was shown that these gratings will provide both high angular selectivity and high spectral selectivity; both of which are unusual for thin reflection holograms. Through the use of these equations and the application of Fourier analysis of these solutions, other characteristics of this grating were also predicted.

Introduction

A hologram is a pattern produced by interference of two coherent beams in a photosensitive medium. In traditional image reproduction, as in a photograph or television picture, only modulus of the amplitude of the original light field is being recorded. In holography, the amplitude and phase of the original wave are reproduced, depicting the original image in perfect three-dimensionality [3]. In addition to image recording, interference patterns can also be recorded as a hologram. A phase hologram is a pattern produced by spatial variations of refractive index in the recording medium. A Bragg grating is a volume phase hologram that is the result of the interference of two plane beams where the thickness of the grating is much more than the reading wavelength. These types of gratings are currently being manufactured using a material known as (PTR) glass.

PTR glass is made from sodium, zinc, aluminum, silicate glass doped with silver ions (Ag^{+}), cerium ions (Ce^{3+}), and fluorine that demonstrates refractive index variations after being exposed to UV radiation and thermal development. When exposed to the UV light, the Ce^{3+} atoms further ionize, giving off an electron becoming Ce^{4+} atoms. Some of these free electrons then combine with the Ag^{+} ions, which become neutral silver (Ag^{0}). At approximately 400°C, the Ag^{0} atoms are able to diffuse in the glass and cluster together, forming silver nanocrystals. When the glass is further heated to approximately 500°C, these silver nanocrystals catalyze the formation of NaF crystals. These NaF crystals cause refractive index variations in the glass. The glass has an approximate refractive index of 1.5 and NaF has an approximate refractive index of 1.3 [1].

Phase volume holograms recorded in PTR glass are not sensitive to optical radiation and the gratings are stable to 400°C. They have a high tolerance to pulsed and continuous wave laser radiation. PTR Bragg gratings have been tested under laser illumination of 100 kW/cm^2 at 1096 nm, with no laser induced damage observed [1]. They have high diffraction efficiency with both angular and spectral selectivity. They are a good alternative for rugged, low cost diffractive optics.

These type of gratings have a wide variety of possible applications: They can be used as wavelength selective filters in wave division multiplexing (WDM) technology of fiber optics networks [4], as optical amplifiers [2], and as wavelength and directional filters in free space optics (FSO). FSO is a line-of-sight technology that uses lasers to provide optical bandwidth connections that can send and receive voice, video, and data information on beams of light.

These gratings are currently being utilized at CREOL in the development of semi-conductor and solid-state lasers. Their robust nature also makes them ideal candidates for use in high-energy laser applications.

Results of previous studies on reflection and transmission gratings with a single hologram recorded in the glass led to the development of the following formulas that govern the diffraction efficiency η of these devices. By definition, diffraction efficiency η is the ratio of the power of the output diffracted wave to the power of the input wave. These formulas may be found in any of numerous books on holography; we will reproduce them as they are shown in "Speckle-Wave Interactions in Application to Holography and Nonlinear Optics" [5].

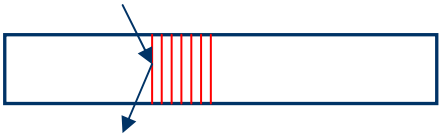

Figure 1. Transmission grating

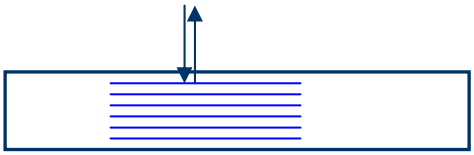

Figure 2. Reflection grating

$$\eta_{trans} = \frac{M^2 \sin^2 \sqrt{X^2 + M^2}}{X^2 + M^2}$$

$$\eta_{reflec} = \frac{M^2 \sin^2 \sqrt{X^2 - M^2}}{X^2 - M^2 \cos^2 \sqrt{X^2 - M^2}}$$

Here the dimensionless parameter M is so-called hologram strength, so that for $M << 1$ the maximum achievable diffraction efficiency η is $\eta = M^2$. Another dimensionless parameter X characterizes possible deviation of hologram in the process of read-out from the optimum Bragg condition. When M is small (<0.3) $\eta_{trans} = \eta_{reflec} = M^2[(\sin X)/X]^2$, but as M gets larger (>0.8) diffraction efficiency is modeled by the above equations. Figure 3 below shows how these relationships become $\eta_{reflec} = \tanh^2 M$ and $\eta_{trans} = \sin^2 M$ when there is zero detuning ($X = 0$) and Figure 4 shows the result as detuning ($X > 0$) is added.

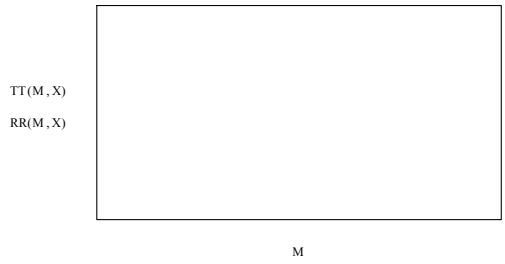

Figure 3. Diffraction Efficiency when X=0. Blue dashed line is reflective efficiency and red solid line is transmission efficiency.

Figure 4. Diffraction Efficiency when X=1.3. Blue vertical line is artifact of computation.

New Research Data

The new Bragg grating that is the subject of this study will have two holograms recorded at 90-degree angles to each other and at a 45-degree angle to the plane of incident waves. These

crossed interference patterns will be present throughout the grating. The following wave propagation patterns will be present in the glass.

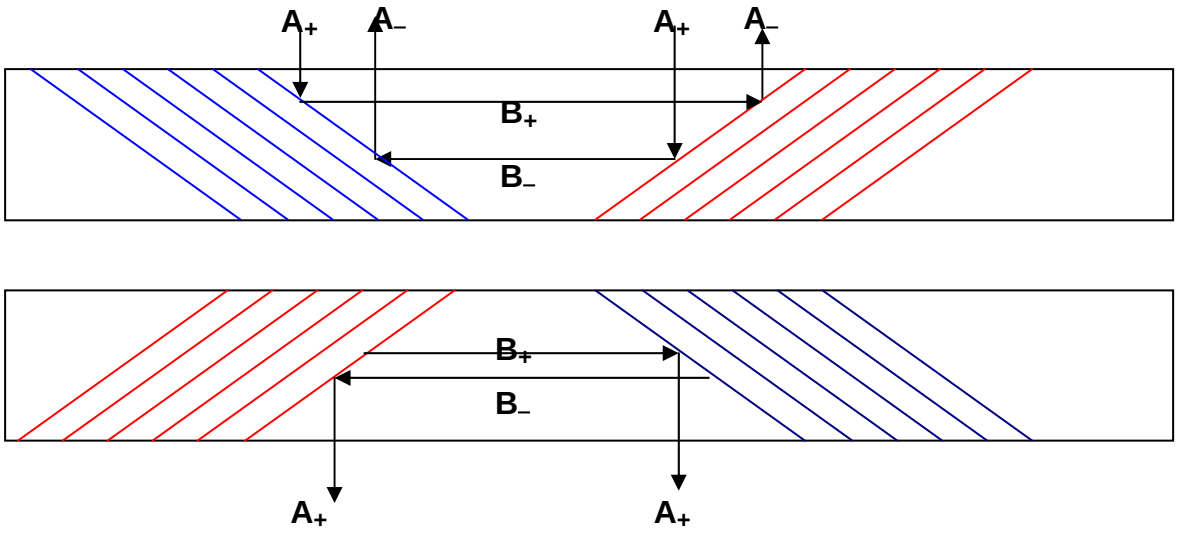

Figure 5. Wave propagation in the new design of the two-grating hologram

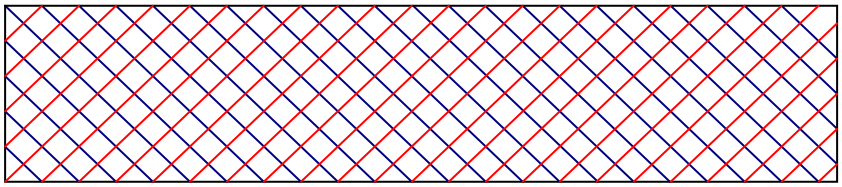

Figure 6. Two gratings as they will appear throughout the glass

The equations that govern the properties of these coupled waves were derived using the Helmholtz equation, which was derived from Maxwell's equations. It was assumed that $\vec{J}_{ext} = 0$.

$$\frac{\partial \vec{D}}{\partial t} + \vec{J}_{ext} = \vec{\nabla} \times \vec{H} \quad \text{(Ampere's Law)} \qquad -\frac{\partial \vec{B}}{\partial t} = \vec{\nabla} \times \vec{E} \quad \text{(Faraday's Law)}$$

$\vec{D} = \varepsilon \vec{E}$ $\vec{B} = \mu \vec{H}$ (Material Relationships).

$\delta \mathbf{D}/\delta t + \mathbf{J}_{ext} =$

This leads to the following transformations:

$$\frac{\partial \vec{D}}{\partial t} = \vec{\nabla} \times \vec{H} \qquad -\frac{\partial \vec{B}}{\partial t} = \vec{\nabla} \times \vec{E}$$

$$\varepsilon \frac{\partial \vec{E}}{\partial t} = \vec{\nabla} \times \vec{H} \;\Rightarrow\; \frac{\partial \vec{E}}{\partial t} = \frac{1}{\varepsilon} \vec{\nabla} \times \vec{H} \qquad -\mu \frac{\partial \vec{H}}{\partial t} = \vec{\nabla} \times \vec{E} \;\Rightarrow\; \frac{\partial \vec{H}}{\partial t} = -\frac{1}{\mu} \vec{\nabla} \times \vec{E}$$

$$\varepsilon \frac{\partial^2 \vec{E}}{\partial t^2} = \vec{\nabla} \times \frac{\partial \vec{H}}{\partial t} \qquad -\mu \frac{\partial^2 \vec{H}}{\partial t^2} = \vec{\nabla} \times \frac{\partial \vec{E}}{\partial t}$$

$$\varepsilon \frac{\partial^2 \vec{E}}{\partial t^2} = -\frac{1}{\mu} \vec{\nabla} \times \left(\vec{\nabla} \times \vec{E} \right) \qquad -\mu \frac{\partial^2 \vec{H}}{\partial t^2} = \frac{1}{\varepsilon} \vec{\nabla} \times \left(\vec{\nabla} \times \vec{H} \right)$$

$$-\mu\varepsilon \frac{\partial^2 \vec{E}}{\partial t^2} = \vec{\nabla} \times \left(\vec{\nabla} \times \vec{E} \right) \qquad -\mu\varepsilon \frac{\partial^2 \vec{H}}{\partial t^2} = \vec{\nabla} \times \left(\vec{\nabla} \times \vec{H} \right)$$

Using the identity $\vec{\nabla} \times \left(\vec{\nabla} \times \vec{A} \right) = -\left(\vec{\nabla} \cdot \vec{\nabla} \right) \vec{A} - \vec{\nabla} \left(\vec{\nabla} \cdot \vec{A} \right)$, these equations become

$$-\mu\varepsilon \frac{\partial^2 \vec{E}}{\partial t^2} = -\left(\vec{\nabla} \cdot \vec{\nabla} \right) \vec{E} - \vec{\nabla} \left(\vec{\nabla} \cdot \vec{E} \right) \qquad -\mu\varepsilon \frac{\partial^2 \vec{H}}{\partial t^2} = -\left(\vec{\nabla} \cdot \vec{\nabla} \right) \vec{H} - \vec{\nabla} \left(\vec{\nabla} \cdot \vec{H} \right).$$

$$\vec{\nabla} \cdot \vec{E} = \vec{\nabla} \cdot \left(\frac{1}{\varepsilon} \vec{D} \right) = \frac{1}{\varepsilon} \vec{\nabla} \cdot \vec{D} = \frac{1}{\varepsilon} \rho_{ext} = 0 \qquad \vec{\nabla} \cdot \vec{H} = \vec{\nabla} \cdot \left(\frac{1}{\mu} \vec{B} \right) = \frac{1}{\mu} \vec{\nabla} \cdot \vec{B} = 0$$

$$\mu\varepsilon \frac{\partial^2 \vec{E}}{\partial t^2} - \left(\vec{\nabla} \cdot \vec{\nabla} \right) \vec{E} = 0 \qquad \mu\varepsilon \frac{\partial^2 \vec{H}}{\partial t^2} - \left(\vec{\nabla} \cdot \vec{\nabla} \right) \vec{H} = 0$$

Further manipulation of the equations leads to d'Alembert's equation.

Using $\mu\varepsilon = \frac{1}{\mathrm{v}^2}$ or $\frac{1}{\mathrm{c}^2}$ if $\varepsilon_o \mu_o$ and $\vec{\nabla} \cdot \vec{\nabla} = \vec{\nabla}^2 = \frac{\partial^2}{\partial x^2} + \frac{\partial^2}{\partial y^2} + \frac{\partial^2}{\partial z^2}$ (Laplacian), we get

$\frac{1}{\mathrm{v}^2} \frac{\partial^2 E}{\partial t^2} - \left(\frac{\partial^2}{\partial x^2} + \frac{\partial^2}{\partial y^2} + \frac{\partial^2}{\partial z^2} \right) E = 0$ (d'Alembert's equation), where E can be $\vec{\mathrm{B}}, \vec{\mathrm{H}}, \vec{\mathrm{D}}$, or $\vec{\mathrm{E}}$.

It is assumed that $E = e^{-i\omega t}$; and since $\frac{\partial^2}{\partial \mathrm{t}} \left(e^{-i\omega t} \right) = -\omega^2 e^{-i\omega t}$, we get the Helmholtz equation.

$$-\left[\frac{\omega^2}{\mathrm{v}^2} E + \left(\frac{\partial^2}{\partial x^2} + \frac{\partial^2}{\partial y^2} + \frac{\partial^2}{\partial z^2} \right) E \right] = 0$$

Since $\mathrm{v} = \frac{c}{n}$, this becomes

$$\left(\frac{\partial^2}{\partial x^2} + \frac{\partial^2}{\partial y^2} + \frac{\partial^2}{\partial z^2} \right) E + \frac{\omega^2}{c^2} n^2 E = 0 .$$

We assume that the total field consists of four waves: A_+, A_-, B_+, B_-: $E(\mathrm{x},\mathrm{z}) = A_+ e^{ikz}, A_- e^{-ikz}, B_+ e^{ikx},$ and $B_- e^{-ikx}$, where $k = \frac{\omega}{c} n$ and $n^2 = (n_o + \delta n)^2$ we get

$$\left(\frac{\partial^2}{\partial z^2} + \frac{\partial^2}{\partial x^2} \right) A_+ e^{ikz} + \frac{\omega^2}{c^2} {n_o}^2 A_+ e^{ikz} + \frac{\omega^2}{c^2} 2 n_o \delta n(x,z) \left(A_+, A_-, B_+, B_- \right) = 0 .$$

By using the Slowly Varying Envelope Approximation (SVEA) method, this equation is then reduced to the following set of differential equations:

$$\frac{\partial A_+}{\partial z} = (-\alpha + is)A_+ + 0 \cdot A_- + i\mu_1 B_+ + i\mu_2 B_- \qquad (1)$$

$$\frac{\partial A_-}{\partial z} = 0 \cdot A_+ + (-\alpha + is)A_- - i\mu_2 B_+ - i\mu_1 B_- \qquad (2)$$

$$\frac{\partial B_+}{\partial z} = i\mu_1 A_+ + i\mu_2 A_- + (-\beta + is)B_+ + 0 \cdot B_- \qquad (3)$$

$$\frac{\partial B_-}{\partial z} = i\mu_2 A_+ - i\mu_1 A_- + 0 \cdot B_+ + (-\beta + is)B_- \qquad (4)$$

where
α (m^{-1}, for amplitude) – attenuation coefficient.
s (m^{-1}) – correction due to spectral detuning.
$\mu_{1,2}$ – coupling coefficient.

We assume A, B is e^{iqx}. Use this in equations 3 and 4, solve for B_+ and B_-, plug these into equations 1 and 2 to get the 2 following differential equations:

$$\frac{\partial A_+}{\partial z} = A_+\left(-\alpha + is - \frac{\mu_1^{\,2}}{\beta + i(q-s)} - \frac{\mu_2^{\,2}}{\beta + i(-q-s)}\right) + A_-\left(-\frac{\mu_1\mu_2}{\beta + i(q-s)} - \frac{\mu_2\mu_1}{\beta + i(-q-s)}\right)$$

$$\frac{\partial A_-}{\partial z} = A_+\left(\frac{\mu_1\mu_2}{\beta + i(q-s)} + \frac{\mu_1\mu_2}{\beta + i(-q-s)}\right) + A_-\left(\alpha - is + \frac{\mu_1^{\,2}}{\beta + i(q-s)} + \frac{\mu_2^{\,2}}{\beta + i(-q-s)}\right)$$

Let us introduce the following notations:

$$Q = \left(-\frac{\mu_1\mu_2}{\beta + i(q-s)} - \frac{\mu_2\mu_1}{\beta + i(-q-s)}\right) \text{ and } P = (-\alpha + is + Q).$$

Then our system of equations for A_+ and A_- takes the form:

$$\frac{\partial A_+}{\partial z} = A_+P + A_-Q$$

$$\frac{\partial A_-}{\partial z} = -A_+Q - A_-P$$

Linear algebra can then be used to produce the solution to these equations by the following:

$$\begin{bmatrix} A_+(z) \\ A_-(z) \end{bmatrix} = \exp(\hat{M}z) \begin{bmatrix} A_+(z=0) \\ A_-(z=0) \end{bmatrix}$$

Eigenvalues $\lambda_{1,2}$ of matrix $\hat{M} = \begin{bmatrix} P & Q \\ -P & -Q \end{bmatrix}$ were found, solving $\det\left(\hat{M} - \hat{1}\lambda\right) = 0$ for λ, to be $\pm(P^2\text{-}Q^2)^{1/2}$. $\exp(\hat{M}z)$ was calculated by the following method, with ρ defined to be $(P^2\text{-}Q^2)^{1/2}$, then redefined as $\exp(\hat{M}z) = \hat{H}$.

$$\exp(\hat{M}z) = e^{\lambda_1 Z}\frac{\hat{M} - \hat{1}\lambda_2}{\lambda_1 - \lambda_2} + e^{\lambda_2 Z}\frac{\hat{M} - \hat{1}\lambda_1}{\lambda_2 - \lambda_{2\ 1}} = \begin{bmatrix} \frac{P}{\rho}\sin(\rho z) + \cos(\rho z) & \frac{Q}{\rho}\sin(\rho z) \\ -\frac{Q}{\rho}\sin(\rho z) & -\frac{P}{\rho}\sin(\rho z) + \cos(\rho z) \end{bmatrix} = \hat{H}$$

Using $\begin{bmatrix} A_+(L) \\ A_-(L) \end{bmatrix} = \begin{bmatrix} H_{11} & H_{12} \\ H_{21} & H_{22} \end{bmatrix}\begin{bmatrix} A_+(z=0) \\ A_-(z=0) \end{bmatrix}$, the reflection and transmission efficiency of the grating can be determined as follows using boundary conditions $A_+(z=0) = 1$ and $A_-(L) = 0$.

$$A_-(L) = \hat{H}_{21}A_+(z=0) + \hat{H}_{22}A_-(z=0) = 0$$

Reflection efficiency: $\eta_{\text{reflec}} = \left|A_-(z=0)\right|^2 = \left|(-\hat{H}_{21}/\hat{H}_{22})\right|^2$

$$A_+(z=L) = \hat{H}_{11}A_+(z=0) + \hat{H}_{12}A_-(z=0)$$

Transmission efficiency: $\eta_{\text{trans}} = \left|A_+(z=L)\right|^2 = \left|\hat{H}_{11} - \left(\hat{H}_{21}/\hat{H}_{22}\right)\hat{H}_{12}\right|^2$

A plot (Figure 7) was generated showing the transmission and reflection efficiencies as a function of grating strength. This plot shows that the efficiency of the transmitted beam decreases at a faster rate than the efficiency of the reflected beam; there is less than 100 percent of the wave energy being accounted for in the graph. This is apparently due to the effect of unlimited propagation of the wave in the z direction in this model. There may need to be an adjustment made to the model to account for a finite distance of the grating in the z direction to get a full accounting of the energy of the beam propagation.

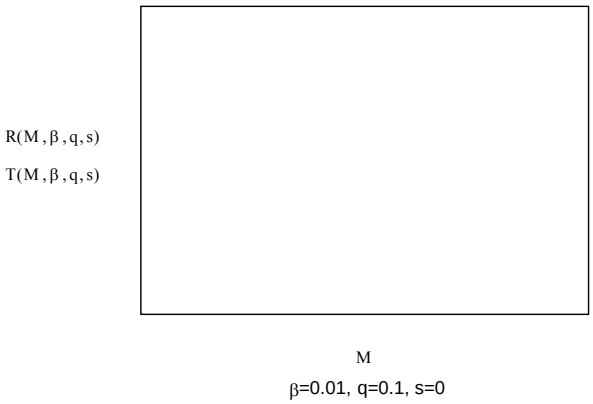

Figure 7. Reflection and transmission efficiency

Using these efficiency formulas and varying the different parameters, the characteristics of the grating can be plotted graphically. This allows for the study of the effects of grating strength, absorption, and detuning parameters on the grating efficiency. Figures 8 and 9 are plots created with the amplitude absorption coefficient $\alpha = 0.0001$ and the detuning factor not being varied set to zero. Let us remind that in the units chosen the thickness of the hologram L was taken to be 1. They show the efficiency dropping off as the parameters vary from the ideal Bragg condition; a good indication of the spectral and angular selectivity of the grating. This holds true for both weak and strong gratings. The plot in Figure 10 shows the relationship between the angular detuning (q) and the spectral detuning (s) as they relate to η_{reflec}. It shows how a loss of efficiency caused by one type of detuning can be offset by a change in the other. This characteristic would be beneficial especially for tunable filters in WDM, where a change in the angle of the grating will be accompanied by a shift in the reflective wavelength band. It would also be very effective in free space optics applications.

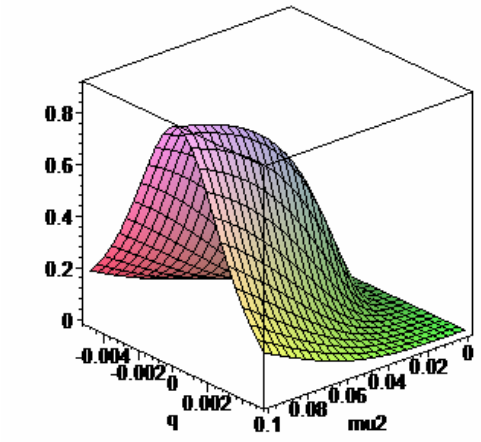

Figure 8. Spectral selectivity, where q is angular detuning and mu2 is grating strength

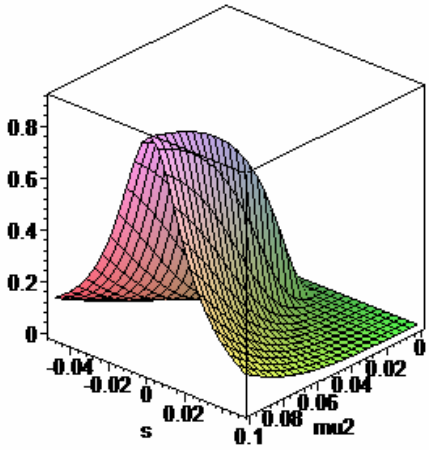

Figure 9. Angular selectivity, where s is spectral detuning and mu2 is grating strength

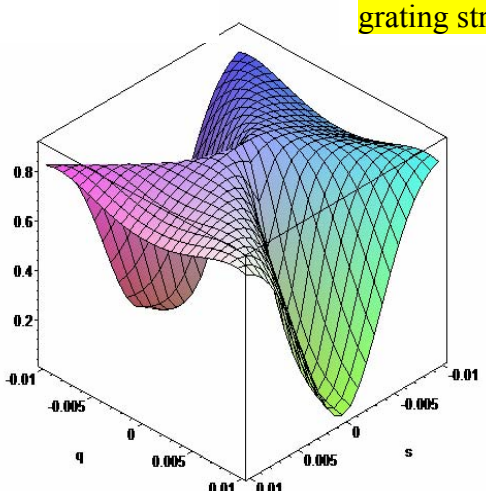

Figure 10. Spectral vs angular Detuning, where q is angular detuning and s is spectral detuning and mu2 is grating strength

Since with e^{iqx} there is linearity and x-shift invariance, a Fourier transform can be used to represent the spatial distribution of the wave throughout the grating in the z direction.

$$A_+(x,z=0) = \exp(iqx)$$
$$A_-(x,z=0) = (-\hat{H}_{21}/\hat{H}_{22})\ \exp(iqx)$$
$$A_+(x,z=0) = \int_{-\infty}^{+\infty} \tilde{A}_+(q,z=0)\cdot \exp(iqx)dq \quad \text{(Fourier transform)}$$
$$A_-(x,z=0) = \int_{-\infty}^{+\infty} \tilde{A}_+(q,z=0)\cdot (-\hat{H}_{21}/\hat{H}_{22})\cdot \exp(iqx)\ dq$$

Let us consider the use of an input Gaussian beam of the form $A_+(x,z=0) = \exp(-x^2/2a^2)$. Here a is the half-width of the beam, δx(Half-Width at a level of e^{-1}, of the intensity at Maximum), or $\delta x(\mathrm{HW}e^{-1}\mathrm{M}) = a$. Parameter a can be varied and the intensity of the reflected light across the surface of the grating can be graphically represented. A couple of examples follow.

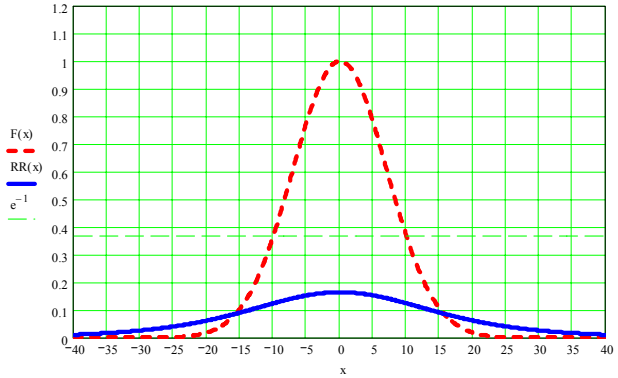

a=10, M=1, β=0.001, s=0

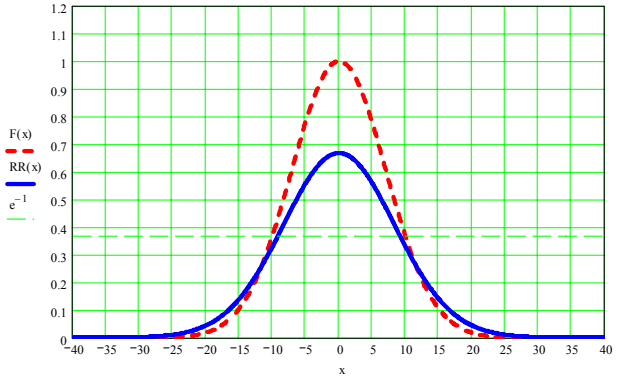

a=10, M=4, β=0.001, s=0

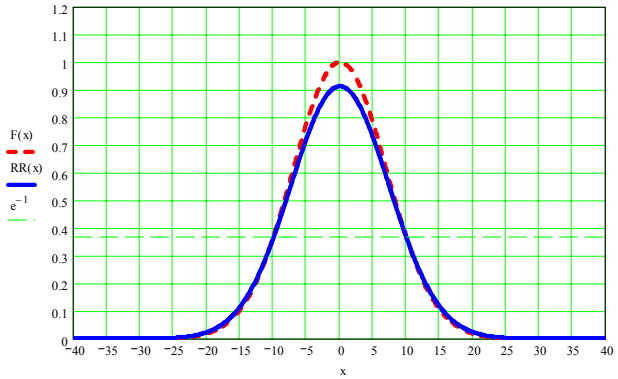

a=10, M=10, β=0.001, s=0

Figure 11. Transverse profile of the reflected beam intensity as grating strength "*M*" is increased, where F(x) (red dashed line) is incident beam intensity and RR(x) is the reflected beam intensity.

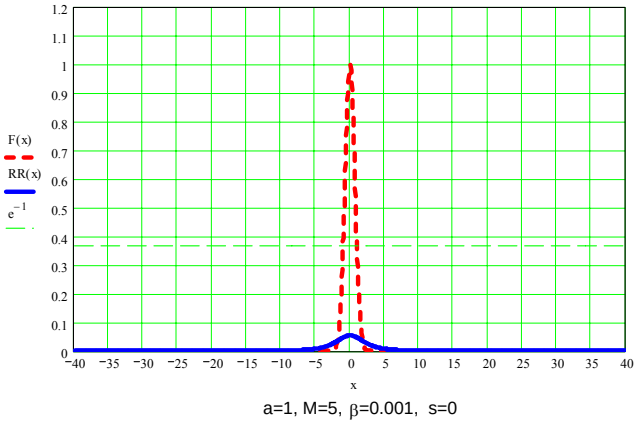

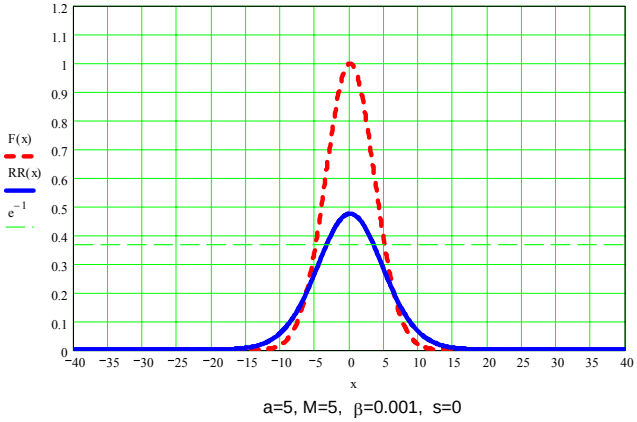

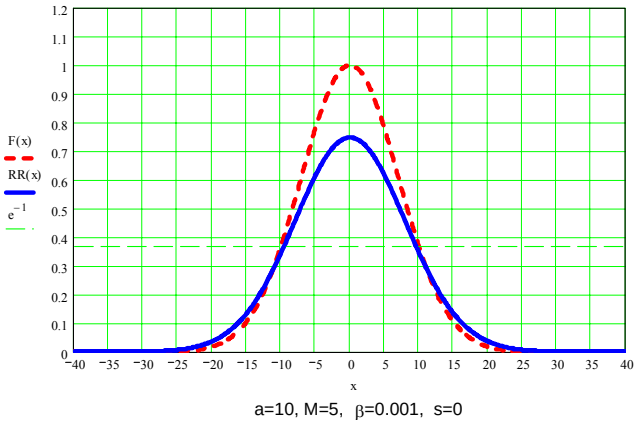

Figure 12. Reflected beam intensity as beam width *a* is increased, where F(x) is incident beam intensity and RR(x) is the reflected beam intensity.

These graphs show that as the variables of grating strength, absorption, detuning, and/or beam width were increased, the amount of "spreading" of the reflected beam will decrease and the reflected beam will more closely approximate the incident beam.

Conclusion

The model still requires a little tweaking to reduce or eliminate the possibility of infinite propagation of the wave in the z-direction. However, it is good enough to indicate that this new configuration of Bragg diffraction grating promises to deliver high angular selectivity and high spectral selectivity, both of which are both unusual for thin reflection holograms. This gives the grating the benefit of, among other things, being used as a tunable filter. The grating does have some spreading of the light under certain conditions. This is offset by its many benefits, and the spreading can be reduced through varying the different parameters that go into the makeup of the grating. There are many applications for these gratings , especially in the realm of communications. At this time, there are no gratings of this type being manufactured. Testing of this theory will have to wait until the time when the gratings are fabricated and available for laboratory experiments.

Acknowledgements:

Dr. Boris Ya Zeldovich - Wave Theory Group/CREOL/UCF

C.C. Tsai - Wave Theory Group/CREOL/UCF

Dr. Glebov - Photoinduced Processing Lab

Dr Craig Siders - Director, Research Experience for Undergraduates/Creol/UCF

References:

[1] Glebov, L.B. "Volume Hologram Recording in Inorganic Glasses." Glass Science and Technology 75 C1 (2002). Verlag der Deutschen Glastechnischen Gesellschaft Frankfurt/Main. Glass and the Photonic Revolution – First International Workshop 2002.

[2] Guy, Martin, Jocelyn Lauzon, Martin Rochette, and Francois Trepanier. "Applications of Bragg Gratings in Optical Amplifiers." TeraXion. nd. July 19, 2004. <http://www.teraxion.com/fr/pdf/articles/ICAPT_2000.pdf>

[3] Hecht, Eugene. "Optics." Pearson Education, Inc (publishing as Addison Wesley). San Francisco. 2002.

[4] Volodin, Boris L., Sergei Dolgy, Elena Melnik, and Vladimir Ban. "Volume Bragg Gratings, a New Platform Technology for WDM Applications." PD-LD, Inc. nd. July 19, 2004 http://www.pd-ld.com/pdf/VBG_PAPER.pdf

[5] Zeldovich, Boris Ya., Alexander V. Mamaev , and Vladimir V. Shkunov. "Speckle-Wave Interactions in Application to Holography and Nonlinear Optics." CRC Press, Inc. Boca Raton. 1995.

Wave Propagation in a Volume Hologram with Multiple Diffraction Gratings

Steven Frederick

Advisor: Dr. Boris Zeldovich

School of Optics/CREOL

University of Central Florida

Abstract

In the last 10 years, Bragg diffraction gratings have been developed at CREOL using photo-thermo-refractive (PTR) glass, which is not sensitive to radiation, temperatures to 400°C, and can withstand high intensity laser beams without damage or change in the Bragg angle. A new type of Bragg grating, composed of two gratings in the same material, at 90 degrees to each other and 45 degrees to the incident wave, is being studied to predict its properties. It was shown that these gratings will provide both high angular selectivity and high spectral selectivity. These are both unusual for thin reflection holograms.

PTR Bragg Gratings

A Bragg grating is a volume phase hologram that contains a pattern produced by spatial variations of refractive index. These variations are produced when photo-thermo refractive (PTR) glass is exposed to UV light and thermally treated. The exposed areas then have a lower refractive index than the surrounding medium.

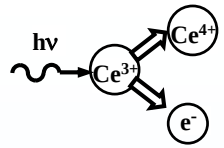

Photo-thermo-crystallization

Courtesy of Dr. Glebov's group

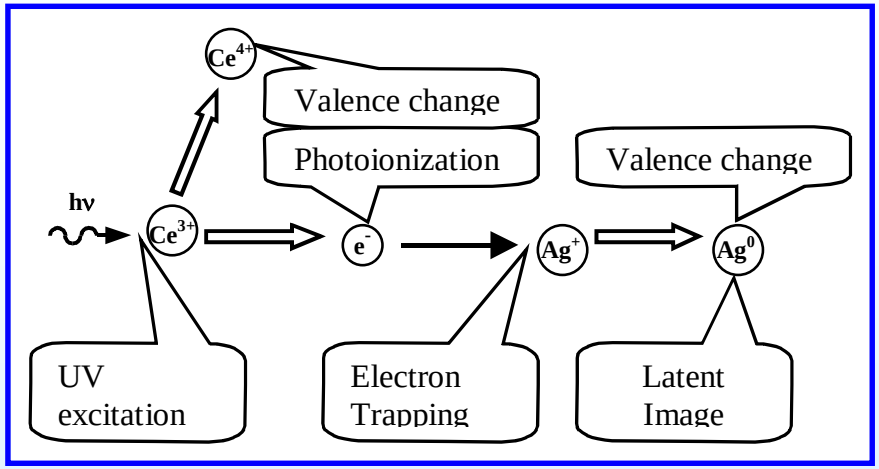

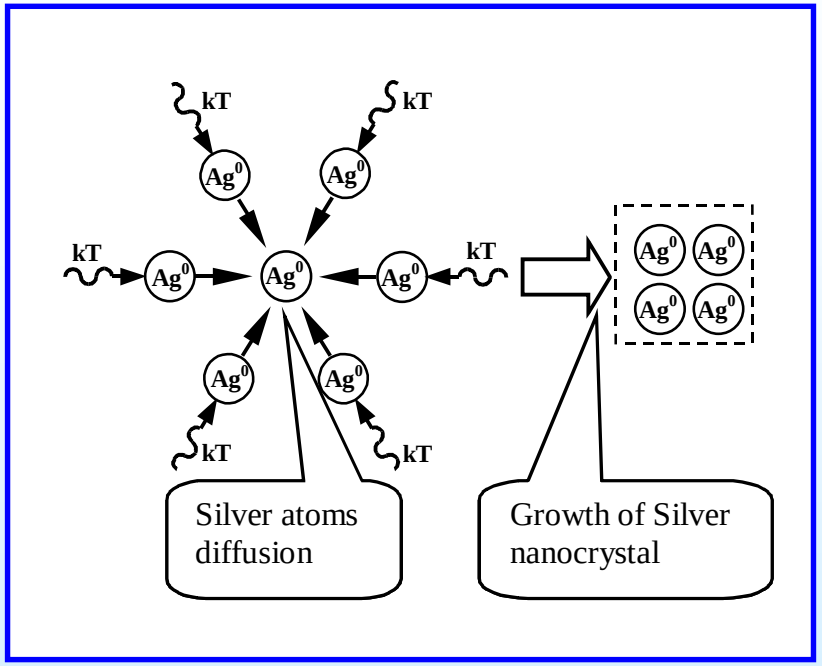

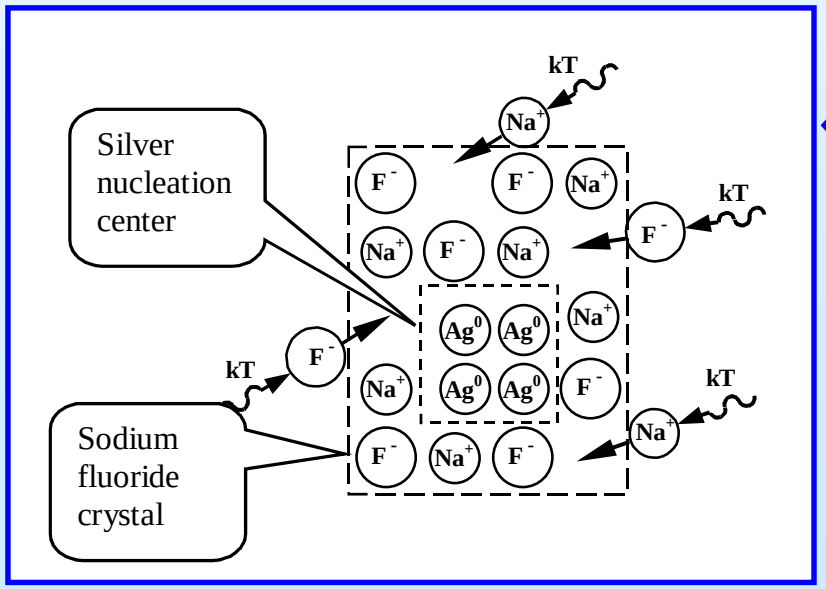

3D image (or hologram) of object is transformed to the phase pattern (refractive index variations) caused by sodium fluoride concentration distribution in accordance with UV intensity distribution in the volume of glass

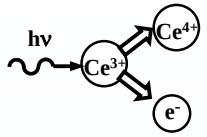

Advantages of PTR Bragg gratings

Courtesy of Dr. Glebov's group

Volume diffractive gratings have been fabricated in photo-thermo-refractive (PTR) glasses with absolute diffraction efficiency above 90 % for the spatial frequency up to 10000 mm^{-1}.

Exposed and developed grating is not sensitive to optical radiation and stable up to 400°C.

Angular selectivity of transmitting gratings down to 0.5 mrad and spectral selectivity below 1 nm were shown.

No laser-induced damage, no thermal lens, no Bragg angle shift, and no significant heating were observed in PTR Bragg grating under illumination of 100 kW/cm^2 at 1096 nm.

Laser-induced damage threshold for 1 ns pulses is above 10 J/cm^2.

This opens the way to a new class of rugged and low cost diffractive optics

Transmission versus Reflective Holograms

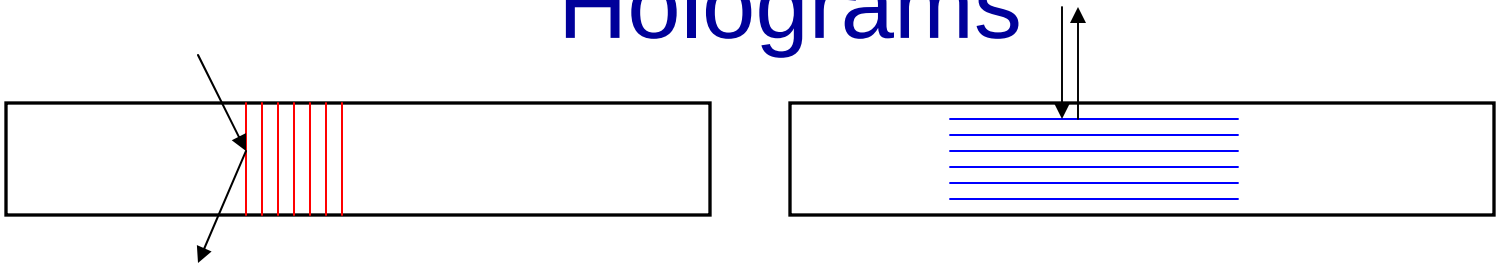

$$\eta_{reflec} = \frac{M^2 \sin^2\sqrt{X^2 - M^2}}{X^2 - M^2\cos^2\sqrt{X^2 - M^2}}$$

$$\eta_{trans} = \frac{M^2 \sin^2\sqrt{X^2 + M^2}}{X^2 + M^2}$$

$$M = \mu \cdot L \qquad X = \Delta \cdot L$$

TT - Transmission

RR - Reflective

X - Detuning from exact Bragg condition

M - Grating strength

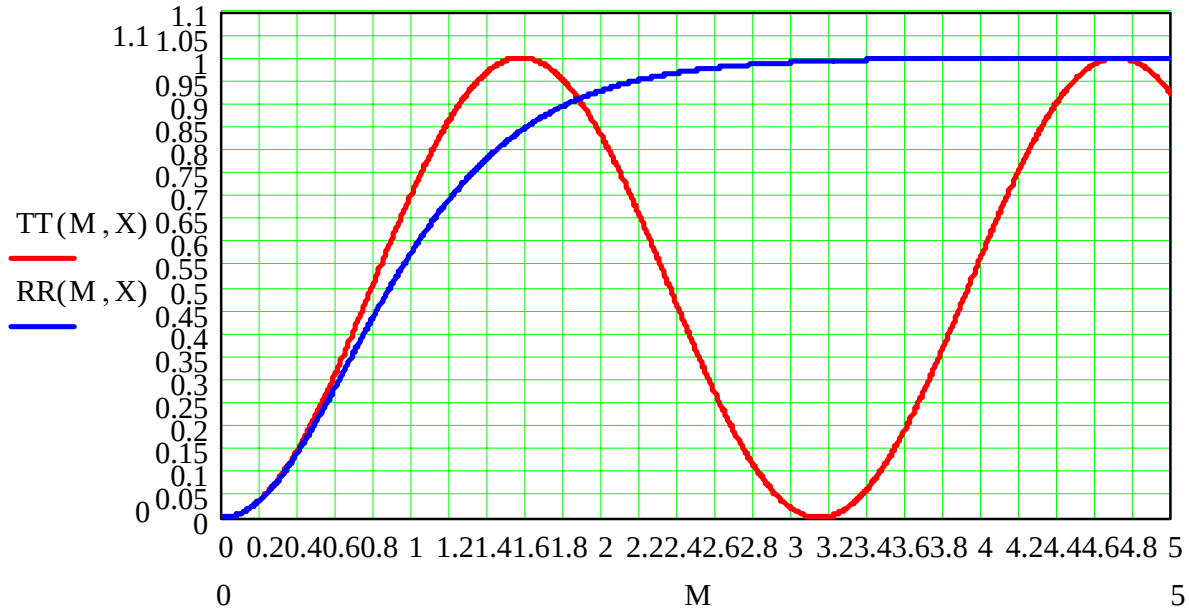

Diffractive Efficiency

Bragg Diffraction Grating to be Made Utilizing PTR Glass

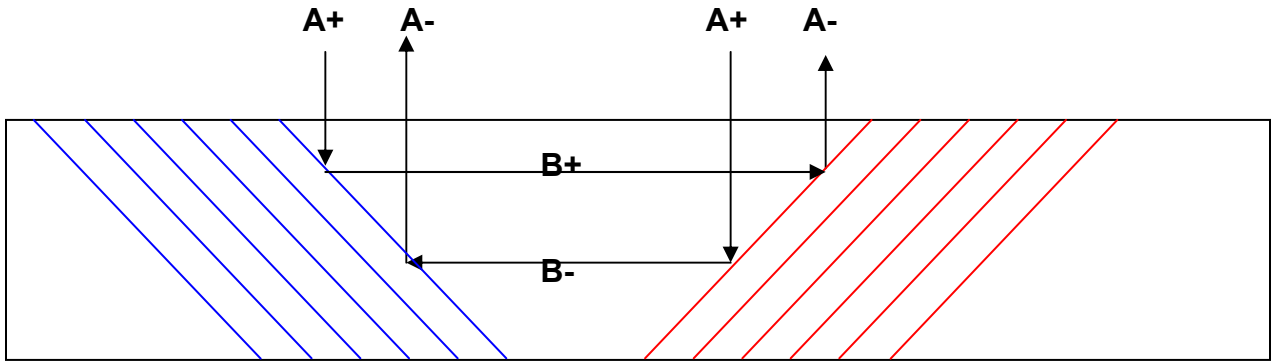

A+, A-, B+, and B- are the waves inside the glass

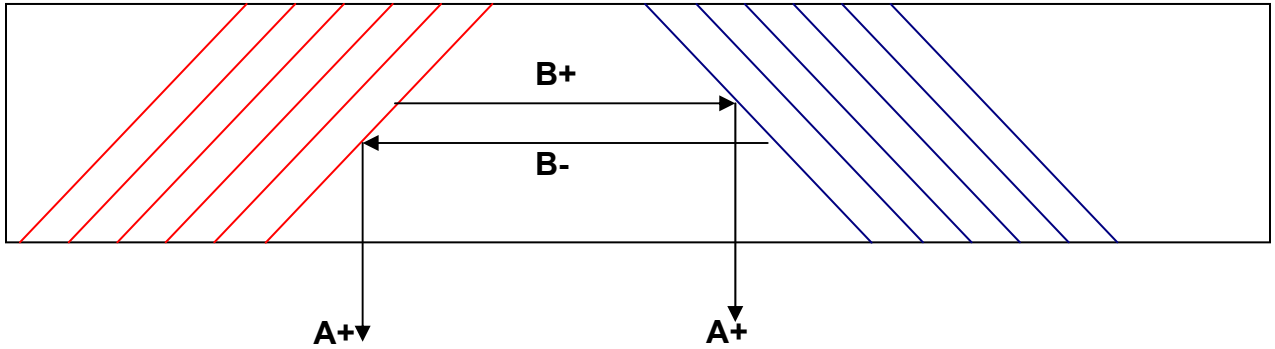

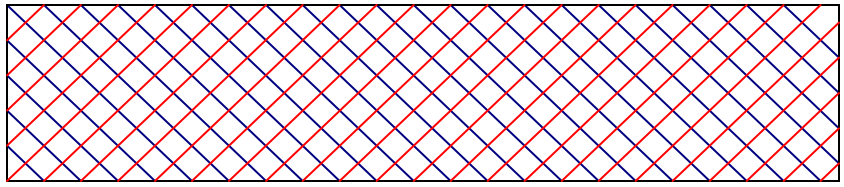

Multiple holograms will be throughout the same piece of glass

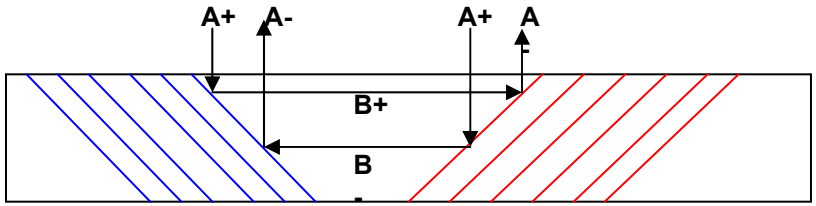

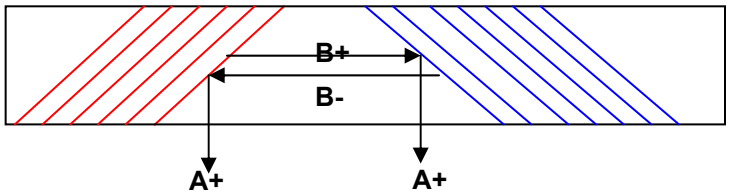

Starting with the Helmholtz Equation:

$$\left(\frac{\partial^2}{\partial x^2}+\frac{\partial^2}{\partial y^2}+\frac{\partial^2}{\partial z^2}\right)E+\frac{\omega^2}{c^2}n^2E=0$$

We let $E(x,z)=A_+e^{ikz}$, A_-e^{-ikz}, B_+e^{ikx}, and B_-e^{-ikx}; $k=\frac{\omega}{c}n$, and by using the Slowly Varying Envelope Approximation (SVEA) method we obtain the following:

$$\left(\frac{\partial^2}{\partial z^2}+\frac{\partial^2}{\partial x^2}\right)A_+e^{ikz}+\frac{\omega^2}{c^2}n_o{}^2A_+e^{ikz}+\frac{\omega^2}{c^2}2n_o\delta n(x,z)\left(A_+,A_-,B_+,B_-\right)=0$$

which reduces to the following set of differential equations:

$$\frac{\partial A_+}{\partial z}=\left(-\alpha+is\right)A_++0\cdot A_-+i\mu_1B_++i\mu_2B_-$$

$$\frac{\partial A_-}{\partial z}=0\cdot A_++\left(-\alpha+is\right)A_--i\mu_2B_+-i\mu_1B_-$$

$$\frac{\partial B_+}{\partial z}=i\mu_1A_++i\mu_2A_-+\left(-\beta+is\right)B_++0\cdot B_-$$

$$\frac{\partial B_-}{\partial z}=i\mu_2A_+-i\mu_1A_-+0\cdot B_++\left(-\beta+is\right)B_-$$

- α and β (m^{-1}, for amplitude), attenuation coefficient
- s (m^{-1}), correction due to spectral detuning
- $\mu_{1,2}$, coupling coefficient

Assume A,B is e^{iqx} (plane wave). Use this in equations 3 and 4, solve for B_+ and B_-, plug these into equations 1 and 2 to get the 2 following differential equations:

$$\frac{\partial A_+}{\partial z}=A_+\left(-\alpha+is-\frac{\mu_1{}^2}{\beta+i(q-s)}-\frac{\mu_2{}^2}{\beta+i(-q-s)}\right)+A_-\left(-\frac{\mu_1\mu_2}{\beta+i(q-s)}-\frac{\mu_2\mu_1}{\beta+i(-q-s)}\right)$$

$$\frac{\partial A_-}{\partial z}=A_+\left(\frac{\mu_1\mu_2}{\beta+i(q-s)}+\frac{\mu_1\mu_2}{\beta+i(-q-s)}\right)+A_-\left(\alpha-is+\frac{\mu_1{}^2}{\beta+i(q-s)}+\frac{\mu_2{}^2}{\beta+i(-q-s)}\right)$$

$$P = -\alpha + is - \frac{\mu_1^{\,2}}{\beta + i(q-s)} - \frac{\mu_2^{\,2}}{\beta + i(-q-s)} \quad \text{and} \quad Q = -\frac{\mu_1\mu_2}{\beta + i(q-s)} - \frac{\mu_2\mu_1}{\beta + i(-q-s)}$$

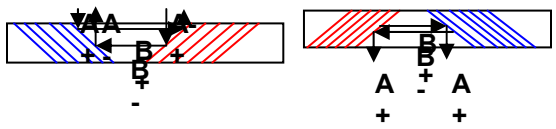

$$\hat{M} = \begin{bmatrix} P & Q \\ -P & -Q \end{bmatrix} \qquad \det\left(\hat{M} - \hat{1}\lambda\right) = 0$$

$$e^{\hat{M}Z} = e^{\lambda_1 Z}\frac{\hat{M} - \hat{1}\lambda_2}{\lambda_1 - \lambda_2} + e^{\lambda_2 Z}\frac{\hat{M} - \hat{1}\lambda_1}{\lambda_2 - \lambda_{2\ 1}} = \hat{H}$$

$$\begin{bmatrix} A_+(z) \\ A_-(z) \end{bmatrix} = e^{\hat{M}Z}\begin{bmatrix} A_+(z=0) \\ A_-(z=0) \end{bmatrix}$$

$$\begin{bmatrix} A_+(z) \\ A_-(z) \end{bmatrix} = \begin{bmatrix} \hat{H}_{11} & \hat{H}_{12} \\ \hat{H}_{21} & \hat{H}_{22} \end{bmatrix}\begin{bmatrix} A_+(z=0) \\ A_-(z=0) \end{bmatrix}$$

Since our boundary conditions are $A_-(L) = 0$ and $A_+(z=0) = 1$, we get:

Reflection Efficiency:

$$A_-(L) = \hat{H}_{21}A_+(z=0) + \hat{H}_{22}A_-(z=0)$$

$$\eta_{reflec} = \left|A_-(z=0)\right|^2 = \left|-\frac{\hat{H}_{21}}{\hat{H}_{22}}\right|^2$$

TransmissionEfficiency:

$$A_+(z=L) = \hat{H}_{11}A_+(z=0) + \hat{H}_{12}A_-(z=0)$$

$$\eta_{trans} = \left|A_+(z=L)\right|^2 = \left|\hat{H}_{11} - \frac{\hat{H}_{21}}{\hat{H}_{22}}\hat{H}_{12}\right|^2$$

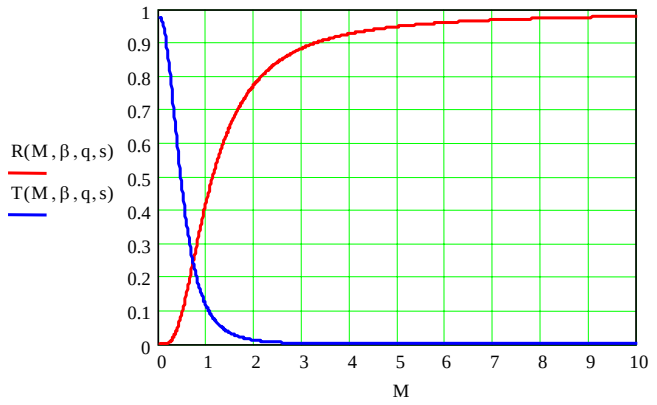

Transmission (T) and reflection (R) efficiency

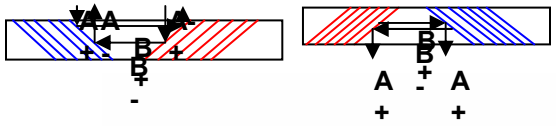

Angular and Spectral Selectivity

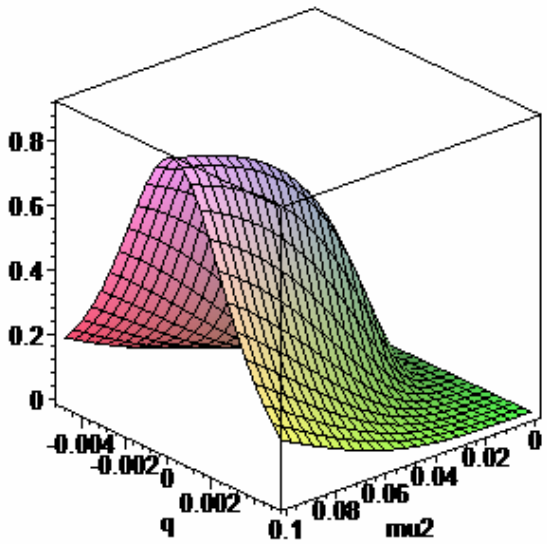

Angular detuning q

α = β = 0.0001
mu1 = mu2

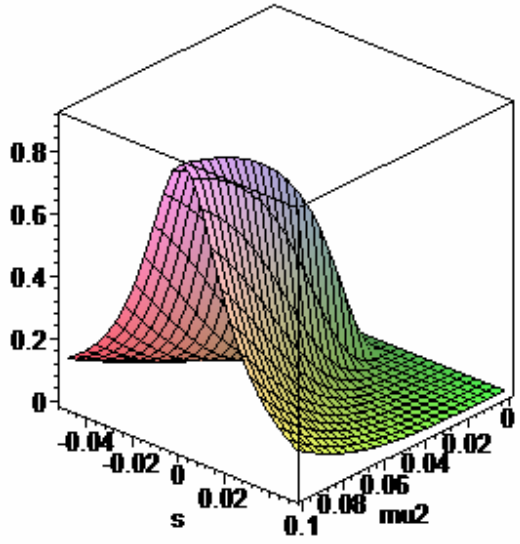

Spectral detuning s

α and β = absorption coefficient
mu1 and mu2 = coupling coeff.
q = angular detuning
s = spectral detuning

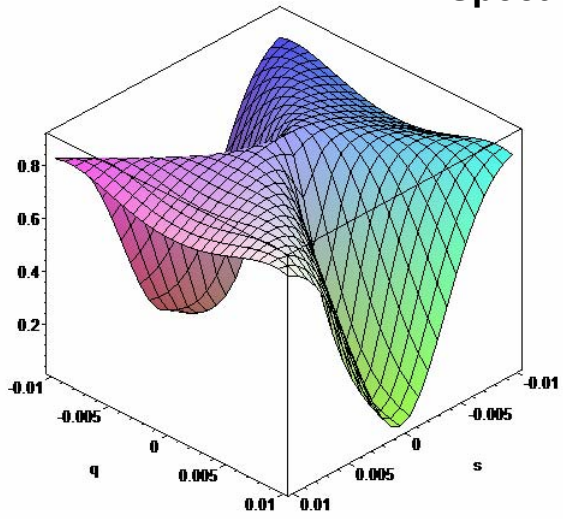

Angular versus spectral detuning
α & β = 0.001, mu1 & mu2 = 0.1

Transverse Profile Calculations

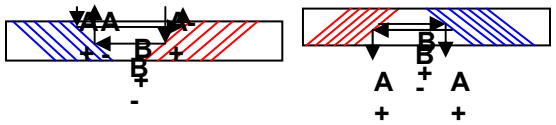

A Fourier transform was used to predict the spatial distribution of light in the grating.

$A_+(x, z=0) = e^{iqx}$

$A_-(x, z=0) = r \cdot e^{iqx}$ (reflection efficiency)

$$A_+(x, z=0) = \int_{-\infty}^{+\infty} \tilde{A}_+(q, z=0) \cdot e^{iqx} dq \quad \text{(Fourier Transform)}$$

$$A_-(x, z=0) = \int_{-\infty}^{+\infty} \tilde{A}_+(q, z=0) \cdot e^{iqx} \cdot r \; dq$$

We use $A_+(x, z=0) = e^{-\frac{x^2}{2a^2}}$, a gaussian beam, and vary the width of the beam "a" to graphically obseve how the light propagates through the glass.

We can also vary other parameters to see the effect it has on the reflected intensity.

Transverse Profile of Reflected Beam

⇑ Hologram Strength "M"

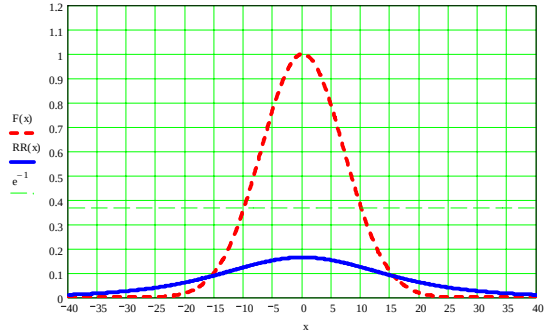

a=10, M=1, β=0.001, s=0

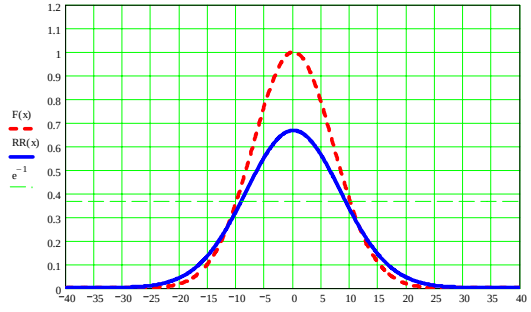

a=10, M=4, β=0.001, s=0

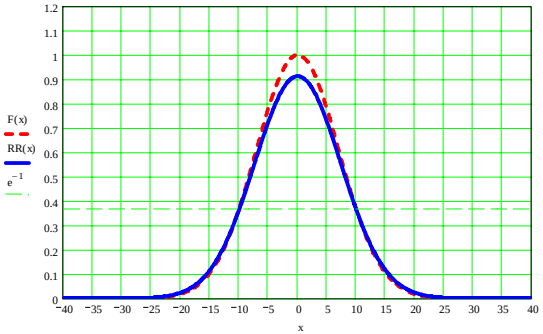

a=10, M=10, β=0.001, s=0

⇑ Beam width "a"

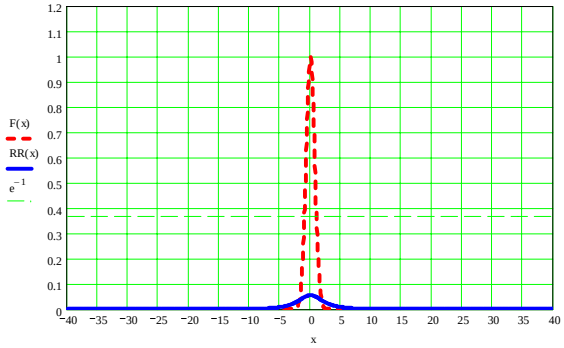

a=1, M=5, β=0.001, s=0

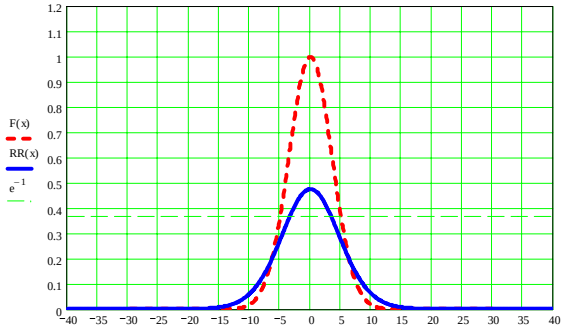

a=5, M=5, β=0.001, s=0

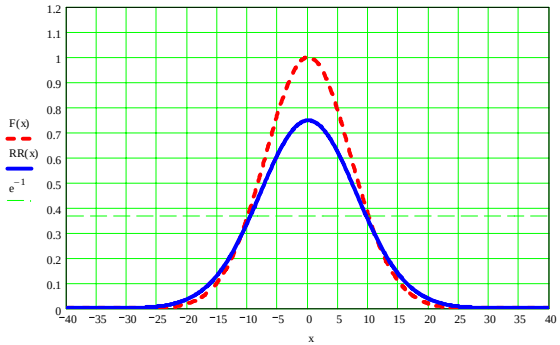

a=10, M=5, β=0.001, s=0

⇑ Detuning "s"

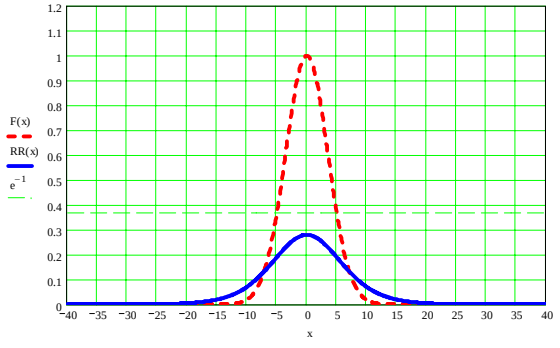

a=5, M=3, β=0.001, s=0

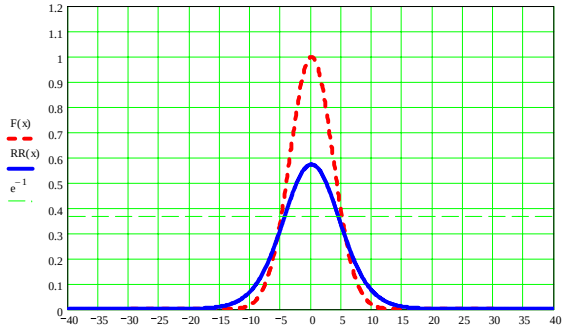

a=5, M=3, β=0.001, s=0.003

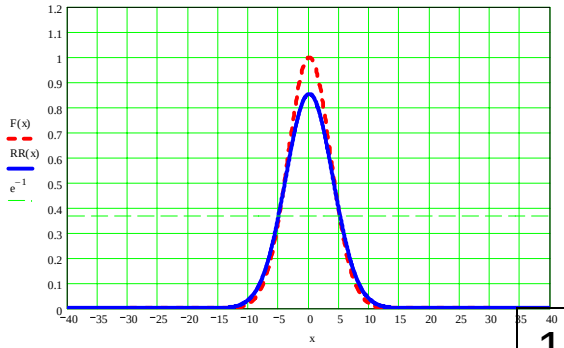

a=5, M=3, β=0.001, s=0.01

Conclusions

- Our new configuration of the grating promises to deliver high angular selectivity and high spectral selectivity; both unusual for thin reflection holograms.
- This model has a small discrepancy due to the unlimited propagation of light allowed in the z direction, compared to finite size in the actual grating.
- There are many possible applications for these type of gratings in Wave Division Multiplexing (WDM) for fiber optic networks, optical amplifiers, and free-space optics.

- Acknowledgements:
  - Dr. Boris Zeldovich - Wave Theory Group, School of Optics/CREOL-UCF
  - Dr Leonid Glebov - Photoinduced Processing Lab, School of Optics/CREOL-UCF
  - Dr Siders – Director of REU program, School of Optics/CREOL-UCF